

# Joint Power Allocation and Path Selection for Multi-Hop Noncoherent Decode and Forward UWB Communications

Marco Mondelli, Qi Zhou, Vincenzo Lottici, and Xiaoli Ma

**Abstract**—With the aim of extending the coverage and improving the performance of impulse radio ultra-wideband (UWB) systems, this paper focuses on developing a novel single differential encoded decode and forward (DF) non-cooperative relaying scheme (NCR). To favor simple receiver structures, differential noncoherent detection is employed which enables effective energy capture without any channel estimation. Putting emphasis on the general case of multi-hop relaying, we illustrate an original algorithm for the joint power allocation and path selection (JPAPS), minimizing an approximate expression of the overall bit error rate (BER). In particular, after deriving a closed-form power allocation strategy, the optimal path selection is reduced to a shortest path problem on a connected graph, which can be solved without any topology information with complexity  $\mathcal{O}(N^3)$ ,  $N$  being the number of available relays of the network. An approximate scheme is also presented, which reduces the complexity to  $\mathcal{O}(N^2)$  while showing a negligible performance loss, and for benchmarking purposes, an exhaustive-search based multi-hop DF cooperative strategy is derived. Simulation results for various network setups corroborate the effectiveness of the proposed low-complexity JPAPS algorithm, which favorably compares to existing AF and DF relaying methods.

**Keywords**—Ultra-wideband (UWB) communications, multi-hop relaying, decode and forward (DF), amplify and forward (AF), noncoherent differential detection, power allocation, path selection.

## I. INTRODUCTION

Ultra-wideband (UWB) impulse radio has been attracting an interest as a strong candidate for short-range high-rate indoor connectivity, low-rate communications with high-resolution ranging, and location-aware wireless sensor networks [1], [2]. Conveying information over a sequence of ultrashort pulses at very low spectral density, several appealing features are promised, such as robustness against multipath, fine timing

resolution, high user capacity, low probability of interception, precise positioning capability, and coexistence with licensed narrowband systems through frequency overlay [3].

**Background.** The harsh multipath propagation conditions typically occurring in wireless environments, however, are a severe factor hindering the pervasive deployment of UWB devices [4]. Exploiting the rich diversity of the UWB channel, indeed, proves to be a very difficult task. The coherent Rake receiver can seemingly solve the problem by collecting a considerable fraction of the received energy scattered over dense multipath [5]. Nevertheless, from a strict implementation viewpoint, the price to be paid consists in a large number of correlator-based fingers and accurate channel estimation, which disagree with the UWB philosophy that calls for as simple as possible receiver processing schemes [6].

In addition, in view of the tight restrictions on the transmitted power spectral density (PSD) issued by the US Federal Communications Commission (FCC) to limit the interference to licensed wireless services [7], an additional key issue for UWB systems consists in the extension of the radio coverage. As a promising answer to this requirement, cooperative communications have been proposed in [8], where some different cooperating strategies are developed and analyzed in terms of outage probability. Henceforward, the cooperative communications concept has stimulated a lot of works: for instance, multi-hop relaying to enhance the capacity of cellular networks [9], relaying optimization based on the maximization of a network sum utility function [10], and opportunistic relaying based on relay selection through packet exchange at network level [11]. Even if the above references have been *de facto* proposed for narrowband systems, they have prompted the applications of cooperative communications to the UWB context as well. The bit error rate (BER) performance analysis for a decode and forward (DF) UWB relaying network is tackled in [12]. Herein, the focus is put on relaying nodes which can adopt different configurations, either single or dual-antenna, and different detection schemes, either coherent or noncoherent, with an equal power allocation strategy. Further, both [13] and [14] consider a network where the nodes are equipped with coherent Rake receiver based on ideally-known channel response. In [13], the design of distributed algebraic space-time codes is addressed to achieve performance gain with the advantage of lower complexity decoding and lower peak-to-average-power-ratio. Alternatively, the two-step approach in [14] is to first derive a cooperative routing strategy to select the highest quality two-hop route in the sense of the asymptotic

Parts of this work were supported by the Georgia Tech Ultrawideband Center of Excellence (<http://www.uwbtech.gatech.edu/>) and by the European Commission in the framework of the FP7 Network of Excellence in Wireless Communications NEWCOM# (Grant agreement no. 318306).

M. Mondelli was with the Sant'Anna School of Advanced Studies and with the Department of Information Engineering, University of Pisa, I-56127 Pisa, Italy. He is now with the School of Computer and Communication Sciences, EPFL, Lausanne, CH-1015, Switzerland.

Q. Zhou and X. Ma are with the School of Electrical and Computer Engineering, Georgia Institute of Technology, GA 30332 Atlanta, USA.

V. Lottici is with the Department of Information Engineering, University of Pisa, I-56122 Pisa, Italy.

Emails: marco.mondelli@epfl.ch; {qzhou32, xiaoli}@ece.gatech.edu; vincenzo.lottici@iet.unipi.it

outage probability (AOP), and then to propose a cooperative scheme, where the received signals from all the active two-hop links are equally weighted and combined together for source-to-destination data transfer.

On the other side, suboptimal yet practical alternatives for effective energy capture have been recently proposed in the form of noncoherent detection schemes [15], [16]. In transmitted reference (TR) systems, the received frame-level waveform, resulting from the information-free pulse sent before data-modulated pulses, is used as noisy template in a correlator unit for data detection [17], [18]. In differential TR (DTR) systems, instead, differential encoding of binary information symbols enables detection using as noisy template the signal waveform received in the previous symbol interval, thus avoiding the wastage of transmit power and data-rate due to the absence of the reference pulses [16], [18]. The noncoherent TR and DTR schemes can gather energy from all the multipath components, thereby skipping costly path-by-path channel estimation.

**Related Work.** Noncoherent receivers have been applied to the context of relaying networks (see e.g., [19], [20], and [21]). In [19], a dual-hop two-way network is discussed wherein two devices exchange information through a single DF relay employing a code-multiplexing TR (CM-TR) signal structure. In [20], a non-cooperative relaying (NCR) strategy is suggested as a way to improve system coverage and performance of multi-hop networks. After multiple differential encoding, the source signal is forwarded to the destination node via a number of subsequent amplify and forward (AF) relays, each performing single differential demodulation. Numerical results indicate promising performance competing even with that offered by some DF schemes. However, a few limitations arise, namely: *i*) the relays have to be ordered before transmission starts, which increases the communication overhead; *ii*) in the specific dual-hop case, the performance is severely degraded when the link connecting either the source with the relay or the relay with the destination exhibits poor quality, and *iii*) the power allocation (PA) across the transmitting nodes is given in closed-form only for the dual-hop and through a sub-optimal recursive algorithm for the multi-hop, whereas the DF case (introduced for performance comparison) is solved through a demanding exhaustive search. In the scheme recently proposed in [21], the signals from both the relayed and direct paths are combined at the destination through a decision rule based on log-likelihood ratio (LLR) test. Significant performance gain is achieved with respect to both the direct transmission using single differential encoding and the NCR scheme of [20], even though the proposed semi-analytical PA strategy makes the extension to the multi-hop case infeasible.

**Rationale of the Proposed Approach and Contribution.** The current paper focuses on single differential encoded DF single-path NCR scheme, in which the intermediate nodes re-encode and transmit again the hard-detected symbols, and proposes a novel relaying technique, referred to as *joint power allocation and path selection* (JPAPS). The presented algorithm optimizes the power allocation coefficients associated to the intermediate nodes and selects the path connecting source to destination capable of minimizing an approximate expression

of the overall BER. Compared with the previous works, the results here show the following distinctive features.

- 1) The power allocation over a path that crosses  $P$  relays is an optimization problem in  $P + 1$  dimensions. A closed-form power allocation strategy is developed which, according to simulation results, yields a BER close to the absolute minimum.
- 2) By performing the optimal path selection through a shortest path search on a connected graph, the computational load required by the JPAPS results to be polynomial in the number of relays of the network. In particular, it is possible to further lower the complexity  $\mathcal{O}(N^3)$  of the exact JPAPS scheme by introducing an approximated path selection algorithm (AJPAPS) which runs in  $\mathcal{O}(N^2)$  without showing a significant performance loss.
- 3) In contrast to the position-based routing techniques discussed in [22], the presented approach does not require information about the network topology and the coordinates of the source and destination.
- 4) A multi-hop CR strategy is also derived, which extends the AF approach in [21] to the DF setting. Herein, each relay forwards the symbols which are detected through first combining the signals received from the previous relays and then thresholding the LLR metrics. However, due to both its overall computational complexity and the significant amount of channel state information (CSI) required, the DF CR scheme will be mainly employed as a performance benchmark.

The effectiveness of the JPAPS algorithm is corroborated by extensive simulation results over typical wireless propagation environments for various network setups. Although derived under a number of approximations, the JPAPS not only favorably compares to the AF and DF relaying techniques proposed in [20], [21], and [12], but also appears to be competitive with the more burdensome DF CR scheme.

**Organization.** The rest of the paper is organized as follows. We start with the description of the model of the relaying network of interest in Sect. II. The proposed NCR JPAPS algorithm is derived in Sect. III, whereas Sect. IV focuses on the optimal CR scheme. Sect. V is devoted to performance comparisons, followed by a few concluding remarks in Sect. VI.

**Notations.** Matrices are in upper case bold while column vectors are in lower case bold,  $(\cdot)^T$  denotes transpose,  $\mathbf{1}_N$  is the  $N \times 1$  vector with all components equal to one,  $\otimes$  denotes convolution, the Q-function is defined as  $Q(x) \triangleq \frac{1}{\sqrt{2\pi}} \int_x^{+\infty} e^{-t^2/2} dt$ , and  $\text{sgn}(x)$  takes value  $+1$  when  $x \geq 0$  and  $-1$  otherwise.

## II. SYSTEM MODEL OVERVIEW

Consider a single-user relay-based UWB network made up by  $N + 2$  devices, namely the source S transmitting the sequence of information symbols, the destination D which collects them, and  $N$  DF relays  $R_i$ ,  $i = 1, \dots, N$ , acting as intermediate nodes to forward information toward the destination. For the ease of notation, let us denote with:

- 1)  $\mathcal{P}(S, R_{i_1}, \dots, R_{i_P}, D)$  the path connecting S to D passing

through the relays  $R_{i_1}, \dots, R_{i_P}$ , with<sup>1</sup>  $0 \leq P \leq N$ ,  $i_1, \dots, i_P \in \{1, \dots, N\}$ , with  $i_j \neq i_k \forall j \neq k \in \{1, \dots, P\}$ ;

- 2)  $\mathcal{L}_{n,m}$  the link existing from node  $n$  to node  $m$ , with  $n \neq m$ ,  $n \in \mathcal{N}_P \triangleq \{S, R_{i_1}, \dots, R_{i_P}\}$  and  $m \in \mathcal{M}_P \triangleq \{R_{i_1}, \dots, R_{i_P}, D\}$ .

Two different DF strategies will be proposed:

- NCR adopting a single path across  $P$  relays, with  $0 \leq P \leq N$ , as described in Sect. III;
- CR exploiting all the  $N$  relays of the network, as described in Sect. IV.

It is worth emphasizing that in the former case the path  $\mathcal{P}$  is chosen among *all the possible routes* according to the actual link propagation conditions, whereas in the CR scheme *all* the  $N$  relays play as intermediate steps on retransmitting the detected symbols.

### A. Signal Model

At the device of index  $n \in \mathcal{N}_P$ , each symbol is transmitted as a block of  $N_f$  consecutive frames, with one pulse  $g(t)$  per frame of sub-nanosecond width  $T_g$  and energy  $E_g \triangleq \int_{-\infty}^{+\infty} g^2(t)dt$ . Without loss of generality, let us adopt the following assumptions.

- A1)  $P$  relays are active, with  $0 \leq P \leq N$ .  
 A2) The source and relays transmit in adjacent time slots, each having duration equal to the symbol interval  $T_s = N_f T_f$ , where  $T_f$  denotes the frame interval which is long enough to avoid the inter-symbol interference (ISI) effect. As a result, the time required to transmit from the source to the destination of the network one information symbol spans  $(P+1)T_s$ , thus ranging from  $T_s$  to  $(N+1)T_s$ .  
 A3) The index  $h_n$ ,  $n \in \mathcal{N}_P$ , designates the slot number, with  $h_S = 0, h_{R_1} = 1, \dots, h_{R_P} = P$ .

Observe that the absence of ISI is a fundamental assumption of the analysis, which is fairly common in the literature (see, e.g., [20], [21]). As concerns the hardware complexity of the long delay line yielded by this requirement, the realization of analog delay components is still under investigation [23], [24]. In contrast, a digital delay element becomes a strong candidate for TR-based UWB systems. Although the main cost of the digital delay element is the very high speed analog-to-digital converters (ADCs), this issue will be addressed by the ongoing development of ADC in the near future.

The signal transmitted by node  $n \in \mathcal{N}_P$  corresponding to a block of  $M$  information symbols can be written as

$$s_n(t) = \sqrt{p_n} \sum_{k=0}^{M-1} \sum_{j=0}^{N_f-1} b_k^{(n)} g[t - jT_f - k(P+1)T_s - h_n T_s], \quad (1)$$

where: i)  $p_n$  is the power allocation coefficient; ii) the channel symbol  $b_k^{(n)}$  results from the differential encoding rule

$$b_k^{(n)} = \begin{cases} b_{k-1}^{(n)} a_k, & \text{if } n = S \\ b_{k-1}^{(n)} \hat{a}_k^{(n)}, & \text{if } n \in \mathcal{N}_P \setminus \{S\} \end{cases} \quad (2)$$

given  $b_{-1}^{(n)}$  as initial value; iii)  $a_k$ ,  $0 \leq k \leq M-1$ , is the sequence of the binary information-bearing symbols transmitted by the source, modeled as independent and identically distributed (i.i.d.) random variables (RVs) equiprobable in  $\{\pm 1\}$ , and iv)  $\hat{a}_k^{(n)}$  is the hard decision taken at the relays having indices  $n \in \mathcal{N}_P \setminus \{S\}$ .

The signal (1) travels through a slow-fading multipath channel connecting node  $n \in \mathcal{N}_P$  with node  $m \in \mathcal{M}_P$ ,  $n \neq m$ , which is assumed to be time-invariant within at least the transmission of two consecutive channel symbols and have  $L_{n,m}$  paths, each with delay  $\tau_i^{(n,m)}$  and uncorrelated normalized gain  $\rho_i^{(n,m)}$ , so that<sup>2</sup>  $\sum_{i=0}^{L_{n,m}-1} [\rho_i^{(n,m)}]^2 = 1$ . Under the assumptions A1)-A3), the signal at the output of the receiver bandpass filter  $h_{BP}(t)$  of bandwidth  $W$  at node  $m$  is

$$r_{n,m}(t) = \sqrt{p_n G_{n,m}} \sum_{k=0}^{M-1} \sum_{j=0}^{N_f-1} b_k^{(n)} \cdot q_{n,m}[t - jT_f - k(P+1)T_s - h_n T_s] + w_{n,m}(t), \quad (3)$$

with  $G_{n,m}$  accounting for both the path loss and the log-normal fading component, where  $G_{n,m}|_{\text{dB}} \triangleq 10 \cdot \log_{10} G_{n,m} = -10\nu \cdot \log_{10} d_{n,m} + \vartheta_{n,m}$ ,  $\nu$  being the path loss exponent depending on the operating scenario,  $d_{n,m}$  the length of the link  $\mathcal{L}_{n,m}$ , and  $\vartheta_{n,m}$  a zero-mean Gaussian RV with variance  $\sigma_F^2$  [25]. The shadowing terms associated to different paths are supposed to be uncorrelated. Furthermore, the received frame-level waveform  $q_{n,m}(t)$  in (3) is expressed as

$$q_{n,m}(t) = \left[ \sum_{i=0}^{L_{n,m}-1} \rho_i^{(n,m)} g(t - \tau_i^{(n,m)}) \right] \otimes h_{BP}(t), \quad (4)$$

and  $w_{n,m}(t)$  denotes filtered zero-mean additive white Gaussian noise (AWGN) with PSD  $\frac{N_0}{2}$  over the bandwidth  $W$  of  $h_{BP}(t)$ .

### B. Symbol Detection

Each receiving node  $m \in \mathcal{M}_P$ , which belongs to the path  $\mathcal{P}$  connecting the source  $S$  with the destination  $D$  across  $P$  intermediate relays, in view of (2) performs noncoherent differential detection without requiring the knowledge of the channel impulse response (CIR) of the link  $\mathcal{L}_{n,m}$ . Due to the time-slotted scheduling, first, the received signal (3) is collected over the non-adjacent slots  $[(k-1)(P+1)T_s + h_n T_s, (k-1)(P+1)T_s + h_n T_s + T_s]$  and  $[k(P+1)T_s + h_n T_s, k(P+1)T_s + h_n T_s + T_s]$ , within which the channel symbols  $b_{k-1}^{(n)}$  and  $b_k^{(n)}$  have been transmitted, respectively. Then, the soft estimate for the information symbol  $a_k$ , i.e.,

<sup>2</sup>The normalized gains are random variables given by the particular channel realization, but the sum of their squares is normalized to 1 at the receiver.

<sup>1</sup>If  $P = 0$ , the direct path  $\mathcal{P}(S, D)$  is considered.

the decision variable, is evaluated as

$$\lambda_{k,P}^{(n,m)} = \sum_{j=0}^{N_f-1} \int_{k(P+1)T_s+h_nT_s+jT_f}^{k(P+1)T_s+h_nT_s+jT_f+T_\varepsilon} r_{n,m}(t) \cdot r_{n,m}[t - (P+1)T_s] dt, \quad (5)$$

where  $T_\varepsilon$  is the integration interval depending on the CIR time span, which is assumed for simplicity to be the same for all the active links.

In order to design the DF relaying network based on either the NCR or CR strategy so that the BER performance at the destination node is optimized, some basic issues arise from the system model perspective.

About the NCR scheme using  $P$  relays out of the  $N$  available ones:

- how the power coefficients  $p_n$ ,  $n \in \mathcal{N}_P$ , have to be chosen for the generic path  $\mathcal{P}$  connecting S to D across  $P$  relays, according to the actual link conditions; and
- how the optimal path can be identified.

About the CR strategy using all the  $N$  relays:

- how to decide the transmit sequence of all relays; and
- how to combine the soft estimates  $\lambda_{k,N}^{(n,m)}$  in (5), which are available at each receiving node.

The next Sect. III and Sect. IV will address the aforementioned issues for the NCR and CR schemes, respectively, in the context of a DF multi-hop network. Significant effort will be put on keeping the required computational load at affordable levels to agree with the UWB philosophy that calls for as simple as possible processing schemes.

### III. JOINT POWER ALLOCATION AND PATH SELECTION FOR NON-COOPERATIVE RELAYING

In this section, we derive the JPAPS algorithm for a DF multi-hop single-path NCR scheme. The steps we will take can be summarized as follows: *i*) definition of the transmission scheduling for the NCR network; *ii*) review of the statistics of the decision variables at the relay and the destination nodes; *iii*) formulation of the PA technique based on a sub-optimal yet efficient equal signal-to-noise ratio (SNR) strategy, given a path crossing  $P$  relays, with  $0 \leq P \leq N$ ; and *iv*) choice of the path that minimizes a high-SNR approximation of the BER performance at the destination node.

#### A. Multi-Hop Single-Path Non-Cooperative Relaying Transmission Scheduling

Let us consider a generic path  $\mathcal{P}(S, R_{i_1}, \dots, R_{i_P}, D)$  connecting S to D through  $P$  relays, composed of the links  $\mathcal{L}_{n,m}$ , with  $n \in \mathcal{N}_P$  and  $m \in \mathcal{M}_P$ ,  $n \neq m$ . The nodes transmit according to the following time-slot (TS) based scheduling:

- TS<sub>1</sub>: S transmits to  $R_{i_1}$ ,
- TS<sub>2</sub>:  $R_{i_1}$  transmits to  $R_{i_2}$ ,
- $\vdots$
- TS <sub>$P+1$</sub> :  $R_{i_P}$  transmits to D.

At node  $m$ , the hard decision

$$\hat{a}_k^{(m)} = \text{sgn} \left\{ \lambda_{k,P}^{(n,m)} \right\} \quad (6)$$

is taken by thresholding the decision variable  $\lambda_{k,P}^{(n,m)}$  given by (5). Then, if  $m \neq D$ , i.e., the destination has not been reached yet, after differential encoding (2) we obtain the symbol  $b_k^{(m)}$  to be retransmitted over the corresponding time slot. Otherwise, if  $m = D$ ,  $\hat{a}_k \triangleq \hat{a}_k^{(D)}$  is the final decision on the information symbol  $a_k$  made by the destination node.

#### B. Statistical Modeling of the Decision Variables

The decision variable  $\lambda_{k,P}^{(n,m)}$  corresponding to the link  $\mathcal{L}_{n,m}$  can be modeled as [15], [18]

$$\lambda_{k,P}^{(n,m)} = \begin{cases} \alpha_{n,m} a_k + \xi_k^{(n,m)}, & \text{if } n = S \\ \alpha_{n,m} \hat{a}_k^{(n)} + \xi_k^{(n,m)}, & \text{if } n \neq S \end{cases}, \quad (7)$$

where  $\xi_k^{(n,m)}$  is a zero-mean Gaussian RV with variance  $\sigma_{n,m}^2$ ,  $\alpha_{n,m}$  is the scaling coefficient, and  $\hat{a}_k^{(n)}$  is the hard decision at node  $n$ . Based on [20], it can be shown that the scaling coefficient  $\alpha_{n,m}$  and the noise variance  $\sigma_{n,m}^2$  are given by

$$\alpha_{n,m} = E_T \delta_{n,m} p_n, \quad (8)$$

$$\sigma_{n,m}^2 = \alpha_{n,m} N_0 + \frac{W N_f T_\varepsilon N_0^2}{2}. \quad (9)$$

Note that in (8)  $E_T \triangleq N_f E_g$  is the energy transmitted when  $p_n = 1$ , and

$$\delta_{n,m} \triangleq G_{n,m} \int_0^{T_\varepsilon} q_{n,m}^2(t) dt \quad (10)$$

denotes the frame-level energy available at the output of the receiver bandpass filter over the interval  $[0, T_\varepsilon]$ .

The frame-level energy parameters  $\delta_{n,m}$  are supposed to be known in order to run the JPAPS algorithm and can be estimated with a sufficiently long preamble of "1" symbols. Indeed, consider the transmission from node  $n$  to node  $m$  using the power coefficient  $p_n = 1$ . Then, the energy captured at the output of the bandpass filter is given by  $\delta_{n,m} + N_0 T_\varepsilon / 2$ , which provides a fairly good estimate of the required parameter, especially if the SNR  $E_T / N_0$  is large enough.

#### C. Power Allocation for a Fixed Relaying Path

In order to formulate the PA rule, we fix a generic path  $\bar{\mathcal{P}}(S, R_{i_1}, \dots, R_{i_P}, D)$  which crosses  $P$  of the  $N$  available relays, and we adopt the following assumptions.

- A4) The available energy  $E_T$  is shared among the source, that transmits  $p_S E_T$ , and the active relays  $R_{i_1}, \dots, R_{i_P}$ , that transmit  $p_{R_{i_1}} E_T, \dots, p_{R_{i_P}} E_T$ , respectively. After defining for simplicity  $R_{i_0} \triangleq S$ , this means that the constraint

$$\sum_{j=0}^P p_{R_{i_j}} = 1 \quad (11)$$

must hold at network level.

- A5) The SNR  $E_T/N_0$  is thought to be sufficiently large so that (9) can be approximated as  $\sigma_{n,m}^2 \simeq \alpha_{n,m}N_0$  and we can assume perfect reconstruction of the frame level energy parameters (10).

Now, let us focus on the BER expression for a given path  $\bar{\mathcal{P}}(S, R_{i_1}, \dots, R_{i_P}, D)$ . Due to the DF-based processing performed by the intermediate nodes, an error is collected at the destination whenever there exists an odd number of errors along  $\bar{\mathcal{P}}$ . Upon neglecting the higher order terms given by the products of Q-functions in view of the assumption A5), we can obtain a high-SNR approximation of the BER metric as

$$\Phi_{\bar{\mathcal{P}}}(\mathbf{p}) = \sum_{\ell=0}^P Q\left(\sqrt{\gamma_{R_{i_\ell}, R_{i_{\ell+1}}}}\right). \quad (12)$$

In plain words,  $\Phi_{\bar{\mathcal{P}}}(\mathbf{p})$  is given by the sum of the BERs of the links which compose  $\bar{\mathcal{P}}$ , where for ease of notation  $R_{i_{P+1}} \triangleq D$ , and from (7)-(9) and assumption A5), the SNR at the output of the link  $\mathcal{L}_{R_{i_\ell}, R_{i_{\ell+1}}}$  can be written as

$$\gamma_{R_{i_\ell}, R_{i_{\ell+1}}} \triangleq \frac{\alpha_{R_{i_\ell}, R_{i_{\ell+1}}}^2}{\sigma_{R_{i_\ell}, R_{i_{\ell+1}}}^2} \simeq \frac{E_T}{N_0} \delta_{R_{i_\ell}, R_{i_{\ell+1}}} p_{R_{i_\ell}}, \quad \ell = 0, \dots, P, \quad (13)$$

with  $\mathbf{p} \triangleq [p_{R_{i_0}}, p_{R_{i_1}}, \dots, p_{R_{i_{P+1}}}]^T$  denoting the vector of the power coefficients to be allocated on the transmitting nodes belonging to the path  $\bar{\mathcal{P}}$ .

Hence, the PA optimization problem (OP), or PA-OP for short, for a given path  $\bar{\mathcal{P}}$  can be formally stated as follows,

$$\begin{cases} \mathbf{p}_o = \arg \min \{\Phi_{\bar{\mathcal{P}}}(\mathbf{p})\} \\ \text{s.t. } \mathbf{1}_P^T \mathbf{p} = 1 \end{cases}. \quad (14)$$

Notice that in the PA-OP (14) both the objective function and the constraint result to be continuous and convex. Thus, the PA-OP is convex as well, and as such, it admits a unique solution [26].

Unfortunately, applying the conventional method of Lagrange multipliers does not yield a closed-form solution, and, as a consequence, some alternatives are required. Due to the convex nature of the PA-OP, a possible numerical method relies on the iterative sub-gradient algorithm [26]. Once the method converges, we are sure that the solution is the optimal one, although this is typically achieved with a slow convergence rate. As the PA-OP has to be solved for all the possible paths  $\bar{\mathcal{P}}$  of the network, it can be definitely concluded that the overall computational load required by this method is unaffordable.

Prompted by these consideration, the idea behind the proposed strategy is *heuristically* based on the fact that the BER performance of a given path is well approximated by the BER of the link experiencing the worst channel conditions. Therefore, the PA-OP is (sub-optimally) solved imposing the equality of the BERs of all the links constituting the path. As the BER of  $\mathcal{L}_{R_{i_\ell}, R_{i_{\ell+1}}}$  is given by  $Q(\sqrt{\gamma_{R_{i_\ell}, R_{i_{\ell+1}}}})$ , the equal-SNR PA (ESPA) strategy sets

$$\gamma_{R_{i_0}, R_{i_1}} = \gamma_{R_{i_1}, R_{i_2}} = \dots = \gamma_{R_{i_P}, R_{i_{P+1}}}, \quad (15)$$

so that all the links will experience the same BER level. Coming into details, after plugging the expression of the SNR (13) into condition (15) and exploiting the constraint (11) of assumption A4), the linear matrix equation

$$\mathbf{\Delta} \mathbf{p} = \mathbf{b} \quad (16)$$

follows, where  $\mathbf{\Delta}$  is the  $(P+1) \times (P+1)$  matrix defined as

$$\mathbf{\Delta} \triangleq \begin{bmatrix} \delta_{R_{i_0}, R_{i_1}} & -\delta_{R_{i_1}, R_{i_2}} & \dots & 0 \\ 0 & \delta_{R_{i_1}, R_{i_2}} & \dots & 0 \\ 0 & 0 & \dots & 0 \\ \vdots & \vdots & \ddots & \vdots \\ 0 & 0 & \dots & -\delta_{R_{i_P}, R_{i_{P+1}}} \\ 1 & 1 & \dots & 1 \end{bmatrix}, \quad (17)$$

and  $\mathbf{b} \triangleq [0, \dots, 0, 1]^T$  is a vector of size  $P+1$ . The solution of (16) leads us to the following proposition.

*Proposition 1 (Power allocation):* Given the frame-level energy parameters  $\delta_{R_{i_\ell}, R_{i_{\ell+1}}}$  for  $\ell \in \{0, \dots, P\}$ , the closed-form sub-optimal ESPA solution for the path  $\bar{\mathcal{P}}$  results as

$$\mathbf{p}_{\text{ESPA}} = \frac{1}{\sum_{\ell=0}^P \delta_{R_{i_\ell}, R_{i_{\ell+1}}}^{-1}} \cdot [\delta_{R_{i_0}, R_{i_1}}^{-1}, \delta_{R_{i_1}, R_{i_2}}^{-1}, \dots, \delta_{R_{i_P}, R_{i_{P+1}}}^{-1}]^T, \quad (18)$$

and accordingly, the minimum BER is approximately expressed by

$$\Phi_{\bar{\mathcal{P}}}(\mathbf{p}_{\text{ESPA}}) = (P+1) \cdot Q\left(\sqrt{\frac{E_T}{N_0} \cdot \left(\sum_{\ell=0}^P \delta_{R_{i_\ell}, R_{i_{\ell+1}}}^{-1}\right)^{-1}}\right). \quad (19)$$

*Proof:* In view of the structure of the matrix  $\mathbf{\Delta}$ , it can be shown that its rows are linearly independent. Hence,  $\det \mathbf{\Delta} > 0$ , and the solution of the linear system is unique. Therefore, plugging (18) into (16) proves that the former is such a solution, from which the minimum BER  $\Phi_{\bar{\mathcal{P}}}(\mathbf{p}_{\text{ESPA}})$  given by (19) follows. ■

A few comments can help on grasping the meaning of Proposition 1.

- 1) Let us consider the dual-hop case ( $N = 1$ , and so  $P = 0$  or  $P = 1$ ), i.e., a relaying network composed of the source S, the relay R, and the destination D, where the possible paths are either the direct  $\mathcal{P}(S, D)$  ( $P = 0$ ) or the relayed one  $\mathcal{P}(S, R, D)$  ( $P = 1$ ). As for the path  $\mathcal{P}(S, R, D)$ , let us assume  $\delta_{R,D} > \delta_{S,R}$ . If the power coefficients were chosen as  $p_S = p_R = 1/2$ , the received energy for the transmission over the link  $\mathcal{L}_{R,D}$  would be greater than that for the transmission over  $\mathcal{L}_{S,R}$ , thus meaning that the BER of the overall path  $\mathcal{P}(S, R, D)$  would be dictated by the worst link  $\mathcal{L}_{S,R}$ . Applying the ESPA scheme, instead, the power coefficients have the form

$$\mathbf{p}_{\text{ESPA}} = [p_S, p_R]^T = \frac{1}{\delta_{S,R} + \delta_{R,D}} \cdot [\delta_{R,D}, \delta_{S,R}]^T, \quad (20)$$

and the received energies for the two transmissions are “equalized”, so that the SNRs at the output of the band-pass filters at R and D result to be the same and equal

to

$$\gamma_{S,R} = \gamma_{R,D} = \frac{E_T}{N_0} \cdot \left( \frac{1}{\delta_{S,R}} + \frac{1}{\delta_{R,D}} \right)^{-1}. \quad (21)$$

Consequently, the overall BER turns out to be

$$\begin{aligned} \Phi_{\mathcal{P}(S,R,D)}(\mathbf{p}_{\text{ESPA}}) &= Q(\sqrt{\gamma_{S,R}}) + Q(\sqrt{\gamma_{R,D}}) \\ &= 2Q\left(\sqrt{\frac{E_T}{N_0} \cdot \left(\frac{1}{\delta_{S,R}} + \frac{1}{\delta_{R,D}}\right)^{-1}}\right). \end{aligned} \quad (22)$$

On the other hand, focusing on the direct path  $\mathcal{P}(S,D)$ , the ESPA solution (18) yields

$$\mathbf{p}_{\text{ESPA}} = [1, 0]^T, \quad (23)$$

i.e., all the available energy is assigned to the source S since the relay R is left unused. Therefore, the corresponding BER results as

$$\Phi_{\mathcal{P}(S,D)}(\mathbf{p}_{\text{ESPA}}) = Q(\sqrt{\gamma_{S,D}}) = Q\left(\sqrt{\frac{E_T}{N_0} \cdot \delta_{S,D}}\right). \quad (24)$$

- 2) The ESPA (18) is a feasible solution for the PA-OP (14) since it satisfies the power constraint. However, due to its sub-optimal nature, it does not ensure to exactly hit the minimum of the objective function  $\Phi_{\mathcal{P}}(\mathbf{p})$  in (12). Nevertheless, the simulation results discussed in Sect. V will interestingly show that the proposed ESPA approach is *near-optimal*, in the sense that it achieves a BER value which is very close to the minimum obtainable through a numerical solution based on exhaustive search.
- 3) Given a transmission path  $\bar{\mathcal{P}}(S, R_{i_1}, \dots, R_{i_P}, D)$ , in order to implement the proposed power allocation, one needs to precompute the vector  $\mathbf{p}_{\text{ESPA}}$  and communicate to each node its power coefficient before transmission starts. As can be seen from the analysis of (18), only the  $P+1$  frame-level energy parameters  $\delta_{R_{i_\ell}, R_{i_{\ell+1}}}$  ( $\ell \in \{0, \dots, P\}$ ) are required to obtain  $\mathbf{p}_{\text{ESPA}}$ , which means that the system complexity is  $\mathcal{O}(N)$ .

#### D. Optimal Path Selection

The JPAPS algorithm can be finalized by selecting the optimal path that minimizes the overall BER performance. Formally speaking, the optimal path selection problem can be formulated as

$$\mathcal{P}_o = \arg \min_{\mathcal{P} \in \mathcal{G}} \{\eta(\mathcal{P})\}, \quad (25)$$

where  $\mathcal{G}$  is the set of all possible paths connecting S with D and the objective function

$$\eta(\mathcal{P}) \triangleq (P+1) \cdot Q\left(\sqrt{\frac{E_T}{N_0} \cdot \left(\sum_{\ell=0}^P \delta_{R_{i_\ell}, R_{i_{\ell+1}}}^{-1}\right)^{-1}}\right) \quad (26)$$

coincides with the (approximate) minimum BER given by (19) employing the ESPA strategy described in Sect. III-C. Since

there exist  $N!/(N-P)!$  different routes to go from S to D passing through  $P$  relays, the cardinality of  $\mathcal{G}$  amounts to  $\sum_{\ell=0}^N N!/\ell!$ . Therefore, solving (25) via a naive exhaustive search requires combinatorial complexity, which even for small  $N$  is clearly infeasible. However, the specific structure of the metric  $\eta(\mathcal{P})$  suggests a much more efficient path selection algorithm, whose rationale relies on: first, finding the set of *candidates* for the optimal path, i.e., one path for each value of  $P$ , with  $0 \leq P \leq N$ , and then, choosing the *global* optimal path in the candidate set as the one which minimizes the metric  $\eta(\mathcal{P})$ . The following proposition clarifies these concepts.

*Proposition 2 (Path selection):* The solution to the minimization problem (25) can be obtained with polynomial complexity  $\mathcal{O}(N^3)$  by means of a two-step procedure.

S1) The  $N+1$  sub-problems

$$\mathcal{P}_{\text{JPAPS}}^{(P)} = \arg \min_{\mathcal{P} \in \mathcal{G}_P} \{\mu(\mathcal{P})\}, \quad 0 \leq P \leq N, \quad (27)$$

are solved adopting the path metric

$$\mu(\mathcal{P}) \triangleq \sum_{\ell=0}^P \delta_{R_{i_\ell}, R_{i_{\ell+1}}}^{-1}, \quad (28)$$

where  $\mathcal{G}_P \triangleq \{\mathcal{P} \mid \mathcal{P} \in \mathcal{G} \text{ and passes through } P \text{ relays only}\}$ .

The result is the set  $\mathcal{C} \triangleq \{\mathcal{P}_{\text{JPAPS}}^{(P)}\}_{P=0}^N$ , which includes the  $N+1$  candidates for the optimal path.

S2) The optimal path follows from

$$\mathcal{P}_{\text{JPAPS}}^{(\text{opt})} = \arg \min_{\mathcal{P} \in \mathcal{C}} \{\eta(\mathcal{P})\}, \quad (29)$$

where  $\eta(\mathcal{P})$  is the metric defined in (26).

*Proof:* Bearing in mind that: *i)* all the paths belonging to  $\mathcal{G}_P$  have  $P$  relays only, and *ii)* the function  $Q(\sqrt{x^{-1}})$  is increasing in  $x$ , then minimizing  $\eta(\mathcal{P})$  for a given  $P$  and  $\frac{E_T}{N_0}$  ratio is equivalent to minimize  $\mu(\mathcal{P})$  in (28). Furthermore,  $\mu(\mathcal{P})$  is an additive metric, i.e., it is the sum of the positive weights  $\delta_{R_{i_\ell}, R_{i_{\ell+1}}}^{-1}$ , one for each link  $\mathcal{L}_{R_{i_\ell}, R_{i_{\ell+1}}}$  belonging to the path  $\mathcal{P}$ . Hence, each sub-problem (27) of step S1 turns into a *shortest path* problem constrained by  $P$  hops with non-negative link metric  $\delta_{R_{i_\ell}, R_{i_{\ell+1}}}^{-1}$ , which can be efficiently solved with polynomial complexity by applying the modified Bellman-Ford (BF) algorithm [27]. More precisely, under the assumption that the relaying network is completely connected, the number of edges of the corresponding graph results to be  $E = \frac{(N+1)(N+2)}{2}$ , and therefore the complexity of step S1 is  $\mathcal{O}(N \cdot E) = \mathcal{O}(N^3)$ . The OP (29) of step S2 consists of selecting the path belonging to  $\mathcal{C}$  that minimizes the original metric  $\eta(\mathcal{P})$  in (26), i.e. of finding the minimum among  $N+1$  elements, and as such, it can be performed in  $\mathcal{O}(N)$ . As a result, the overall complexity of the procedure is  $\mathcal{O}(N^3)$ . ■

Just to exemplify the path selection algorithm, let us focus again on the dual-hop network considered in Sect. III-C, wherein the possible paths are the direct  $\mathcal{P}(S,D)$  ( $P=0$ )

and the relayed one  $\mathcal{P}(S, R, D)$  ( $P = 1$ ). From (22) and (24), the metric (26) evaluated for the relayed path amounts to

$$\eta[\mathcal{P}(S, R, D)] = 2Q \left( \sqrt{\frac{E_T}{N_0} \cdot \left( \frac{1}{\delta_{S,R}} + \frac{1}{\delta_{R,D}} \right)^{-1}} \right), \quad (30)$$

whereas that for the direct one is

$$\eta[\mathcal{P}(S, D)] = Q \left( \sqrt{\frac{E_T}{N_0} \cdot \delta_{S,D}} \right). \quad (31)$$

Therefore, the JPAPS algorithm reduces to the binary testing

$$\mathcal{P}_{\text{JPAPS}}^{(\text{opt})} = \begin{cases} \mathcal{P}(S, R, D), & \eta[\mathcal{P}(S, R, D)] < \eta[\mathcal{P}(S, D)] \\ \mathcal{P}(S, D), & \text{otherwise} \end{cases}. \quad (32)$$

The meaning of (32) can be intuitively explained as follows. Let us assume that  $\mathcal{P}(S, D)$  is not reliable, for example due to a large distance between S and D or to shadowing. This signifies that the BER of  $\mathcal{P}(S, D)$  will be greater than that of  $\mathcal{P}(S, R, D)$ . As a result, the JPAPS algorithm according to the values of  $\eta[\mathcal{P}(S, D)]$  and  $\eta[\mathcal{P}(S, R, D)]$  will correctly choose the relayed path and use the intermediate relay R. Vice versa, whenever  $\delta_{S,R}$  or  $\delta_{R,D}$  is so small that the BER associated to  $\mathcal{P}(S, R, D)$  is higher than that of  $\mathcal{P}(S, D)$ , the JPAPS algorithm will select the direct path  $\mathcal{P}(S, D)$ . In both cases, the path selection diversity is properly exploited, thus contributing to enhance the connectivity between source and destination.

### E. Approximated Path Selection

In order to reduce the overall computational complexity, the path selection algorithm can be suitably approximated, as showed in the following corollary.

*Corollary 1 (Approximated path selection):* The approximated version of the JPAPS algorithm, or AJPAPS for short, finds an approximation to the minimization problem (25) via the OP

$$\mathcal{P}_{\text{AJPAPS}}^{(\text{opt})} = \arg \min_{\mathcal{P} \in \mathcal{G}} \{ \mu(\mathcal{P}) \}, \quad (33)$$

which can be solved in  $\mathcal{O}(N^2)$ .

*Proof:* Since the metric  $\mu(\mathcal{P})$  defined in (28) is additive on the links belonging to a given path  $\mathcal{P}$ , the OP (33) is equivalent to an unconstrained shortest path problem with non-negative link costs (see also Figure 1), which can be efficiently solved through the Fibonacci-heap-based Dijkstra algorithm with complexity  $\mathcal{O}(N^2)$  [28]. ■

A couple of comments about Corollary 1 can be of help.

- 1) In the case of dual-hop network ( $N = 1$ ), the AJPAPS algorithm reduces to

$$\mathcal{P}_{\text{AJPAPS}}^{(\text{opt})} = \begin{cases} \mathcal{P}(S, R, D), & \text{if } \delta_{S,R}^{-1} + \delta_{R,D}^{-1} < \delta_{S,D}^{-1} \\ \mathcal{P}(S, D), & \text{otherwise} \end{cases}. \quad (34)$$

- 2) The AJPAPS algorithm represents a good performance-versus-complexity tradeoff. Indeed, as shown in Sect. V, the BER performance offered by AJPAPS is very similar to that of the JPAPS algorithm, yet requiring a lower order of computational load.

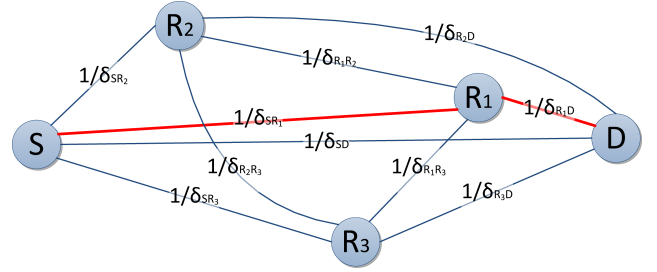


Fig. 1. The AJPAPS algorithm reduces the path selection to an unconstrained shortest path problem with non-negative link costs.

## IV. COOPERATIVE RELAYING

We develop in this section a multi-hop CR scheme in which each relay of the network retransmits toward the destination the recovered symbol, obtained by first combining the received signals from the previously transmitting nodes and then thresholding the LLR corresponding to the soft estimates (5). The following points will be discussed: *i*) definition of the transmission scheduling for the CR network; *ii*) evaluation of the LLR for a given relay, and *iii*) choice of the power coefficients to be employed at the network devices to optimize the BER performance at the destination node.

### A. Multi-Hop Cooperative Relaying Transmission Scheduling

Referring to Figure 2, let us consider the relaying network composed of the source S,  $N$  intermediate relays  $R_1, \dots, R_N$ , and the destination D. Given an ordering of the  $N$  relays, transmissions take place according to the following TS-based scheduling:

- TS<sub>1</sub>: S transmits to  $R_1, \dots, R_N, D$
- TS<sub>2</sub>:  $R_1$  transmits to  $R_2, \dots, R_N, D$
- ⋮
- TS <sub>$N+1$</sub> :  $R_N$  transmits to D.

Defining for notational simplicity  $R_{N+1} \triangleq D$ , at the node of index  $R_j \in \mathcal{M}_N$ , the  $k$ -th symbol is recovered by applying the optimal decision rule

$$\hat{a}_k^{(R_j)} = \text{sgn} \left\{ \Lambda(\boldsymbol{\lambda}_{k,N}^{(R_j)}) \right\}, \quad 1 \leq j \leq N+1, \quad (35)$$

where  $\boldsymbol{\lambda}_{k,N}^{(R_j)} \triangleq [\lambda_{k,N}^{(S,R_j)}, \lambda_{k,N}^{(R_1,R_j)}, \dots, \lambda_{k,N}^{(R_{j-1},R_j)}]^T$  is the  $j$ -dimensional vector including the soft estimates collected in the time intervals TS<sub>1</sub>, TS<sub>2</sub>,  $\dots$ , TS <sub>$j$</sub>  from the links  $\mathcal{L}_{S,R_j}, \mathcal{L}_{R_1,R_j}, \dots, \mathcal{L}_{R_{j-1},R_j}$ , and  $\Lambda(\boldsymbol{\lambda}_{k,N}^{(R_j)})$  is the LLR corresponding to  $\boldsymbol{\lambda}_{k,N}^{(R_j)}$ , as evaluated in Sect. IV-B. After recovering the symbol  $\hat{a}_k^{(R_j)}$  from (35), if  $j \neq N+1$  differential encoding (2) yields the channel symbol  $b_k^{(R_j)}$  to be retransmitted again. Otherwise, if  $j = N+1$ ,  $\hat{a}_k \triangleq \hat{a}_k^{(R_{N+1})}$  is the final decision taken by the destination node on the information symbol  $a_k$ .

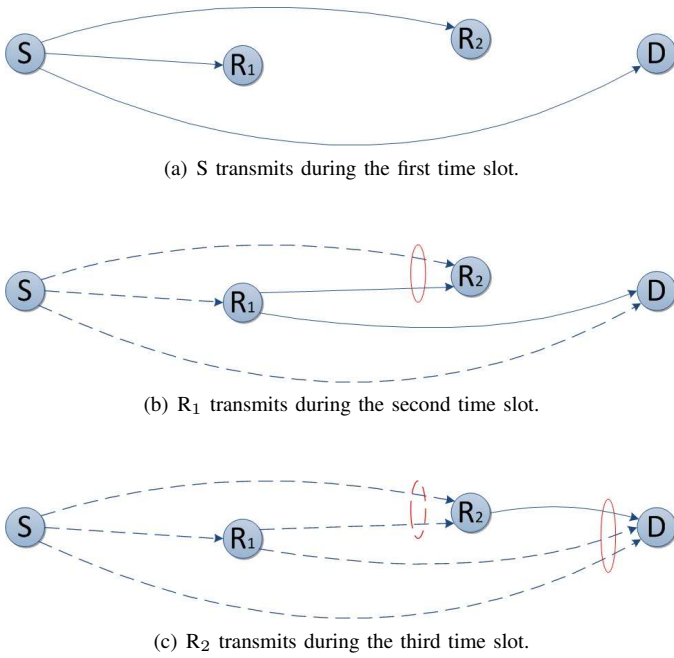


Fig. 2. Multi-hop cooperative relaying (\$N = 2\$).

### B. Evaluation of the LLR Metric

The LLR evaluated at the node \$R\_j\$ is defined as

$$\Lambda(\boldsymbol{\lambda}_{k,N}^{(R_j)}) \triangleq \ln \frac{f_{\lambda}(\boldsymbol{\lambda}_{k,N}^{(R_j)} | a_k = 1)}{f_{\lambda}(\boldsymbol{\lambda}_{k,N}^{(R_j)} | a_k = -1)}, \quad (36)$$

where \$f\_{\lambda}(\boldsymbol{\lambda}\_{k,N}^{(R\_j)})\$ is the joint probability density function (PDF) of \$\boldsymbol{\lambda}\_{k,N}^{(R\_j)}\$. The metric (36) is computed in the following proposition.

*Proposition 3 (Metric evaluation for the CR scheme):*

Under the assumptions A1) (with \$P = N\$) and A2), the LLR \$\Lambda(\boldsymbol{\lambda}\_{k,N}^{(R\_j)})\$, \$1 \leq j \leq N + 1\$, can be written as

$$\Lambda(\boldsymbol{\lambda}_{k,N}^{(R_j)}) = \frac{2\alpha_{S,R_j}}{\sigma_{S,R_j}^2} \lambda_{k,N}^{(S,R_j)} + \sum_{i=1}^{j-1} \Omega(\lambda_{k,N}^{(R_i,R_j)}), \quad (37)$$

with

$$\Omega(\lambda_{k,N}^{(R_i,R_j)}) \triangleq \ln \frac{\cosh\left(\frac{\alpha_{R_i,R_j}}{\sigma_{R_i,R_j}^2} \lambda_{k,N}^{(R_i,R_j)} + \varphi_{R_j}\right)}{\cosh\left(\frac{\alpha_{R_i,R_j}}{\sigma_{R_i,R_j}^2} \lambda_{k,N}^{(R_i,R_j)} - \varphi_{R_j}\right)}, \quad (38)$$

and approximated as

$$\Lambda(\boldsymbol{\lambda}_{k,N}^{(R_j)}) \simeq Z_{k,N}^{(j)} \triangleq \frac{2\alpha_{S,R_j}}{\sigma_{S,R_j}^2} \lambda_{k,N}^{(S,R_j)} + \sum_{i=1}^{j-1} \omega(\lambda_{k,N}^{(R_i,R_j)}), \quad (39)$$

with

$$\omega(\lambda_{k,N}^{(R_i,R_j)}) \triangleq \left| \frac{\alpha_{R_i,R_j}}{\sigma_{R_i,R_j}^2} \lambda_{k,N}^{(R_i,R_j)} + \varphi_{R_j} \right| - \left| \frac{\alpha_{R_i,R_j}}{\sigma_{R_i,R_j}^2} \lambda_{k,N}^{(R_i,R_j)} - \varphi_{R_j} \right|, \quad (40)$$

where \$\varphi\_{R\_j} \triangleq \frac{1}{2} \ln \frac{1 - p\_{eR\_j}}{p\_{eR\_j}}\$, \$p\_{eR\_j} \triangleq \Pr\{\hat{a}\_k^{(R\_j)} \neq a\_k\}\$ being the BER at the node \$R\_j\$.

*Proof:* After setting \$R\_0 \triangleq S\$ for simplicity of notation, since the soft estimates at node \$R\_j \in \mathcal{M}\_N\$, i.e., \$\lambda\_{k,N}^{(R\_0,R\_j)}, \lambda\_{k,N}^{(R\_1,R\_j)}, \dots, \lambda\_{k,N}^{(R\_{j-1},R\_j)}\$, are independent from each other, the LLR in (36) turns out to be

$$\Lambda(\boldsymbol{\lambda}_{k,N}^{(R_j)}) = \sum_{i=0}^{j-1} \ln f_{\lambda}(\lambda_{k,N}^{(R_i,R_j)} | a_k = 1) - \sum_{i=0}^{j-1} \ln f_{\lambda}(\lambda_{k,N}^{(R_i,R_j)} | a_k = -1). \quad (41)$$

Exploiting (7)-(9) and defining \$p\_{eR\_j} \triangleq \Pr\{\hat{a}\_k^{(R\_j)} \neq a\_k\}\$, the conditional marginal PDF \$f\_{\lambda}(\lambda\_{k,N}^{(R\_i,R\_j)} | a\_k)\$ is given by

$$f_{\lambda}(\lambda_{k,N}^{(R_i,R_j)} | a_k) = \frac{1}{\sigma_{R_i,R_j} \sqrt{2\pi}} \begin{cases} \exp\left\{-\frac{[\lambda_{k,N}^{(R_i,R_j)} - \alpha_{R_i,R_j} a_k]^2}{2\sigma_{R_i,R_j}^2}\right\}, & i = 0 \\ p_{eR_j} \exp\left\{-\frac{[\lambda_{k,N}^{(R_i,R_j)} + \alpha_{R_i,R_j} a_k]^2}{2\sigma_{R_i,R_j}^2}\right\} + (1 - p_{eR_j}) \cdot \\ \cdot \exp\left\{-\frac{[\lambda_{k,N}^{(R_i,R_j)} - \alpha_{R_i,R_j} a_k]^2}{2\sigma_{R_i,R_j}^2}\right\}, & 1 \leq i \leq j-1 \end{cases} \quad (42)$$

Upon replacing (42) into (41), the exact expression of the LLR (37)-(38) can thus be obtained. Furthermore, applying the Jacobi approximation, i.e., \$\ln(e^x + e^y) \simeq \max\{x, y\}\$, the approximations in (39)-(40) follow. ■

Some remarks can be given about the multi-hop CR scheme.

- 1) The \$N\$ available relays have to be pre-ordered so that transmissions comply with the TS-based scheduling procedure outlined in Sect. IV-A. Since there exist \$N!\$ different ways of sorting \$N\$ relays, however, an exhaustive search looking for the ordering that enables the best performance appears infeasible even for small \$N\$.
- 2) While the NCR JPAPS algorithm requires only partial CSI in the form of the frame-level energy parameters \$\delta\_{n,m}\$ defined in (10), with \$n \in \mathcal{N}\_N\$ and \$m \in \mathcal{M}\_N\$, \$n \neq m\$, in the CR scheme the model parameters \$\alpha\_{R\_i,R\_j}\$ and \$\sigma\_{R\_i,R\_j}^2\$, with \$0 \leq i \leq j-1\$ and \$1 \leq j \leq N+1\$, have to be pre-computed together with an estimate of the BER level for all the nodes. As a result, the overall computational complexity of the CR is much higher than that of the JPAPS scheme.



### C. Power Allocation for Multi-Hop Cooperative Relaying

The optimal power allocation strategy is far more demanding for the CR approach than for the NCR JPAPS scheme.

In analogy with the dual-hop AF CR technique proposed in [21], a possible option could be based on the solution of the OP

$$\begin{cases} \mathbf{p}_o = \arg \min \{ \text{SNR}_{\text{CR}}(\mathbf{p}) \} \\ \text{s.t. } \mathbf{1}_{N+1}^T \mathbf{p} = 1 \end{cases}, \quad (43)$$

where  $\mathbf{p} \triangleq [p_{R_0}, p_{R_1}, \dots, p_{R_{N+1}}]^T$  and the objective function

$$\text{SNR}_{\text{CR}}(\mathbf{p}) \triangleq \frac{E^2\{Z_{k,N}^{(N+1)}\}}{\text{Var}\{Z_{k,N}^{(N+1)}\}} \quad (44)$$

is the effective SNR at the destination node, based on the RV  $Z_{k,N}^{(N+1)}$  given by (39) with  $j = N + 1$ . Unfortunately, differently from the AF CR scheme of [21], the PA strategy defined in (43)-(44) proves ineffective. Indeed, in the current DF CR scheme, the soft estimates included in  $Z_{k,N}^{(N+1)}$ , i.e.,  $\lambda_{k,N}^{(R_j, R_{N+1})}$  with  $0 \leq j \leq N$ , cannot be modeled as Gaussian RVs, but instead as mixtures of Gaussian RVs, because of the presence of the hard decisions  $\hat{a}_k^{(R_j)}$ .

In order to find an alternative power allocation strategy, let us observe that, from a heuristic point of view, the best path coming into a given relay, say  $R_j$ , dominates its performance. Hence, it can be argued that a good approximation of the BER at the node  $R_j$ , i.e.,  $p_{e_{R_j}}$ , is just given by the minimum among all the BERs pertaining to the admissible paths, namely those going from S to  $R_j$ ,  $R_1$  to  $R_j$ ,  $\dots$ ,  $R_{j-1}$  to  $R_j$ . Hence, setting  $p_{e_{R_0}} = 0$  as an initial condition, after discarding the higher order terms given by the products of Q-functions in line with the high-SNR assumption A5), the recursive equation

$$p_{e_{R_j}} = \min_{i \in \{0, 1, \dots, j-1\}} \{ p_{e_{R_i}} + Q(\sqrt{\gamma_{R_i, R_j}}) \} \quad (45)$$

allows to evaluate the sequence  $p_{e_{R_j}}$ ,  $1 \leq j \leq N$ , of the BER at the relay nodes  $R_1, R_2, \dots, R_N$ , together with the BER at the destination node  $p_{e_D} \triangleq p_{e_{R_{N+1}}}$ . Assuming as objective function  $p_{e_D}$  from (45), we are thus led to formulate the OP for the PA strategy in the CR scenario

$$\begin{cases} \mathbf{p}_o = \arg \min \{ p_{e_D}(\mathbf{p}) \} \\ \text{s.t. } \mathbf{1}_{N+1}^T \mathbf{p} = 1 \end{cases}. \quad (46)$$

The analogy between the OP (14) and that in (46) suggests that a good approximated solution of the latter can be found by exploiting the ESPA strategy outlined in Sect. III-C. Then, solving (46) yields the sequence  $p_{e_{R_j}}$ ,  $1 \leq j \leq N$ , which is eventually employed to evaluate the LLR metrics (37)-(38) or their approximate versions (39)-(40).

## V. SIMULATION RESULTS

In this section, the effectiveness of the JPAPS and AJPAPS schemes is verified through numerical simulations over realistic multipath wireless environments for various network configurations. The simulations have been performed by means

of the numerical computing environment MATLAB. The performance figure is quantified by the BER at the destination node as a function of the  $E_g/N_0$  ratio with  $E_g$  and  $N_0$  being defined in Sect. II.

### A. Benchmark Schemes

The following schemes will be taken as performance benchmarks:

- 1) source-destination direct transmission (DT) with single differential encoding;
- 2) DF NCR with single differential encoding and equal power allocation (DF-NCR-EP), as proposed in [12];
- 3) DF NCR with single differential encoding and the optimal power allocation (DF-NCR-OP) proposed in Sect. III-C;
- 4) DF CR with single differential encoding and equal power allocation (DF-CR-EP), as discussed in Sect. IV-B;
- 5) DF CR with single differential encoding and optimal power distribution (DF-CR-OP), in which the power allocation coefficients are optimized numerically by making them vary in the interval  $[0, 1]$  and choosing the values that yield the minimum BER;
- 6) AF CR with multiple differential encoding and the optimal power allocation strategy (AF-CR-OP) proposed in [21];
- 7) AF NCR with multiple differential encoding and the optimal power allocation strategy (AF-NCR-OP) proposed in [20];
- 8) DF NCR with single differential encoding and joint power allocation and path selection (JPAPS), as proposed in Sect. III-C and III-D;
- 9) DF NCR with single differential encoding and approximate joint power allocation and path selection (AJPAPS), as proposed in Sect. III-E.

Note that, if not otherwise specified, all the performance comparisons among the above benchmark schemes will be carried out taking as a reference the BER level of  $10^{-3}$ .

### B. Simulation Setup

In the setup considered for the numerical simulations, the source node transmits bursts of  $M$  binary information-bearing symbols, where the symbol interval is made up of  $N_f = 2$  frames with an ultra-short pulse  $g(t)$  per frame, the so-called monocycle, defined as

$$g(t) = \left[ 1 - 4\pi \left( \frac{t - \vartheta}{\varphi} \right)^2 \right] e^{-2\pi[(t - \vartheta)/\varphi]^2}, \quad (47)$$

with  $\vartheta = 0.35$  ns and  $\varphi = 0.2877$  ns. The pulse and frame durations are  $T_g = 0.7$  ns and  $T_f = 70$  ns, respectively, and accordingly, the symbol interval equals  $T_s = N_f T_f = 140$  ns. No time-hopping code is employed, the bandwidth of the receiver band-pass filter is set to  $W = 5$  GHz, and the integration interval is  $T_\varepsilon = 5.25$  ns [20].

The channel model is assumed to be time-invariant within each burst, but randomly varying from burst to burst according to the IEEE 802.15.3a-CM1 model [25], [29]. The path loss

exponent is  $\nu = 3$ , and the deviation of the log-normal fading component is  $\sigma_F = 2.5$ . Thus, according to the time-spread of the channel model and the value of the frame interval  $T_f$ , the ISI effect can be considered negligible.

We focus on five network configurations (NCs), as depicted in Figure 3, differing for both the number of relays and their disposition.

- NC1: line configuration with  $N = 1$  relay between the source S and the destination D;
- NC2: isosceles triangle configuration with  $N = 1$  relay;
- NC3: line configuration with  $N = 2$  relays between the source S and the destination D;
- NC4: square configuration with  $N = 2$  relays positioned on the vertices;
- NC5: generic configuration formed by a square room of side 4 meters, with the source S and the destination D placed on a couple of diagonal vertices, and  $N = 10$  relays, one of which is placed in the middle and the other ones are uniformly and randomly distributed inside.

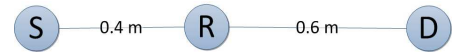
### C. Check for the Power Allocation Adopted for the JPAPS Algorithm

Figures 4-5 deal with the transmission of a single burst of  $M$  consecutive information symbols over a given realization of the CIRs and channel gains, adopting the configurations NC1, NC2 ( $N = 1$ ) and NC3 ( $N = 2$ ). In both figures, the BER is plotted against the  $N$  power allocation coefficients<sup>3</sup> by making them vary in the interval  $[0, 1]$  with the step-size of  $10^{-2}$ . For the single relay system analyzed in Figure 4,  $M = 10^6$ , and two values of  $E_g/N_0$  are chosen for each of the two dual-hop scenarios, in order to obtain a minimum BER close to  $10^{-2}$  and  $10^{-4}$ . For the configuration with two relays in Figure 5,  $M = 10^5$  and  $E_g/N_0 = 12$  dB, so that the minimum BER is close to  $10^{-3}$ . In all the cases, the BER performance achieved using the PA coefficients given by (21) and (18) for the case  $N = 1$  and  $N = 2$  respectively, is very close to that obtained through exhaustive search.

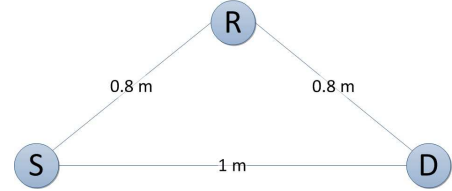
### D. BER Performance for Dual-Hop Configurations

Figures 6-7 compare the schemes listed in Sect. V-A for the single relay configurations NC1 and NC2, respectively. For a specific value of the  $E_g/N_0$  ratio,  $10^4$  different bursts are transmitted, each conveying  $M = 10^3$  information symbols and experiencing a different realization of the wireless propagation channels. In particular, for each realization of the transmission, independent channel gains are generated and the CIRs of the different links are selected randomly from a set of 100 sample channel responses given by [29].

In Figure 6, it can be noted that the DF-NCR-EP [12] offers a gain of about 4 dB at the target BER of  $10^{-3}$  with respect to the conventional DT. In contrast, in Figure 7, the DT slightly outperforms the DF-NCR-EP by approximately 1 dB. The reason is simply that the scenario NC1 of Figure 6



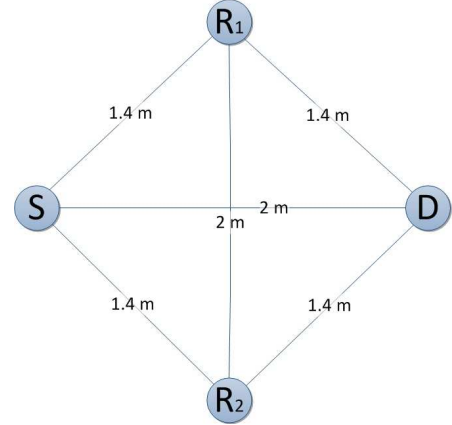
(a) Line configuration with  $N = 1$  relay (NC1).



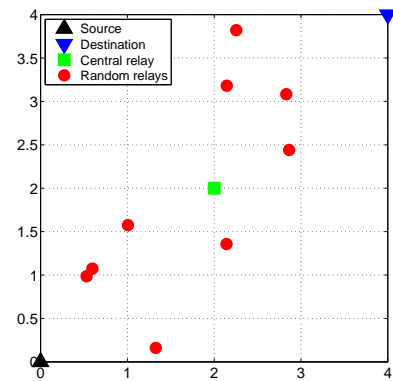
(b) Triangle configuration with  $N = 1$  relay (NC2).



(c) Line configuration with  $N = 2$  relays (NC3).



(d) Square configuration with  $N = 2$  relays (NC4).



(e) Generic configuration with  $N = 10$  relays (NC5).

<sup>3</sup>The value of the  $(N + 1)$ -st power coefficient is obtained from the power constraint equation.

Fig. 3. Network configurations.

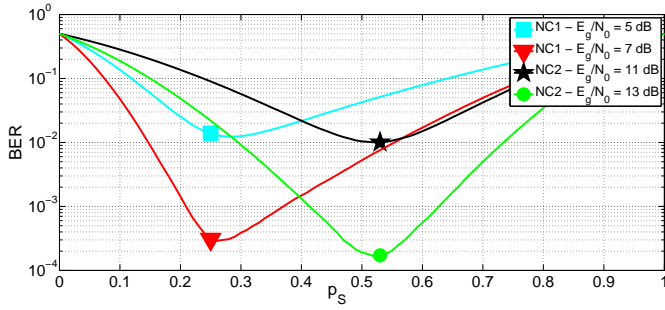


Fig. 4. BER as a function of the power allocation coefficient of the source S for NC1 and NC2.

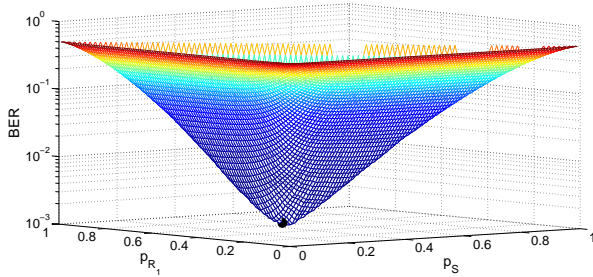


Fig. 5. BER as a function of power allocation coefficients of the source S and relay  $R_1$  for NC3.

favors the relayed path  $\mathcal{P}(S, R, D)$ , while for NC2 in Figure 7  $\mathcal{P}(S, R, D)$  turns out to be unfavorable. Anyway, it can be argued from both the figures that the proposed JPAPS scheme: *i*) coincides with the approximated version AJPAPS, which, however, shows one less order of complexity; *ii*) yields a performance improvement of 3 dB with respect to the DF-NCR-EP and the DT in Figures 6 and 7, respectively, and *iii*) offers a gain of 1 dB with respect to the AF-CR-OP [21] for both NC1 and NC2, and of about 2 dB (4.5 dB) for NC1 (NC2) with respect to the AF-NCR-OP [20]. It has to be noted that, although the JPAPS requires a much lower computational load (and the AJPAPS even less), it outperforms the DF-CR-EP by 1.5 dB (1 dB) for NC1 (NC2), and it incurs in a negligible 0.4 dB loss compared to the DF-CR-OP in which the PA coefficients are found by an exhaustive search, i.e., performing the transmission for each possible couple of power coefficients (with a fixed step size) and then selecting the one that minimizes the BER. In addition, remark that, even if in general the AF schemes amplify also the noise along with signal and, therefore, are outperformed by the DF relaying systems [30], the AF-CR-OP yields better results than the DF-NCR-EP and the DF-CR-EP due to its different encoding and power allocation strategy.

### E. BER Performance for Multi-Hop Configurations

Figures 8-9 address two scenarios with  $N = 2$  relays corresponding to NC3 and NC4, respectively. As in NC1, in the multi-hop line configuration NC3 of Figure 8, a more favorable path exists as well, i.e., the relayed path  $\mathcal{P}(S, R_1, R_2, D)$ .

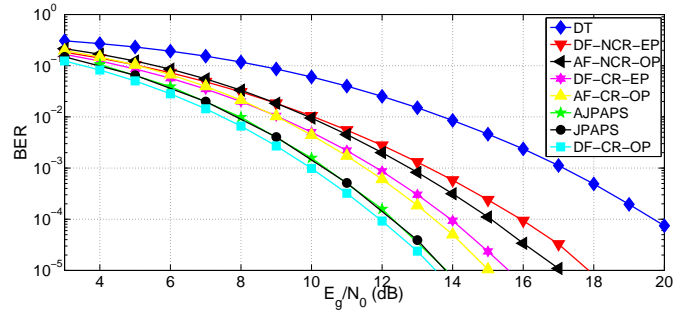


Fig. 6. BER as a function of the SNR for various transmission schemes (NC1).

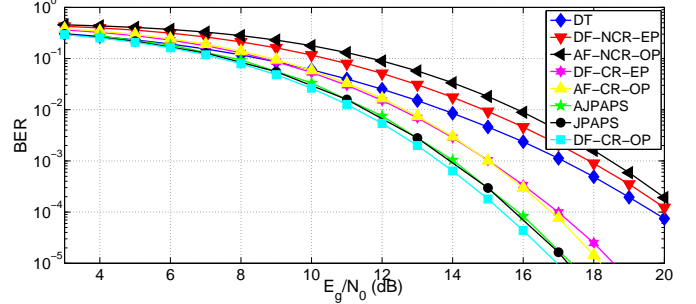


Fig. 7. BER as a function of the SNR for various transmission schemes (NC2).

Thus, the DF-NCR-EP based on  $\mathcal{P}(S, R_1, R_2, D)$  shows a performance gain of 4 dB over the DF-NCR-EP based on  $\mathcal{P}(S, R_1, D)$  and even of 7 dB with respect to the DT. On the other hand, for the square configuration NC4 of Figure 9,  $\mathcal{P}(S, R_1, R_2, D)$  is no longer the most convenient path, and the DF-NCR-EP that employs that route is outperformed by the DT and the DF-NRC-EP based on  $\mathcal{P}(S, R_1, D)$ , which come out to be almost equivalent. By applying the proposed JPAPS (or the AJPAPS, which again yields the same error performance), a considerable gain of about 4 dB is enabled on the DF-NCR-EP for NC3, which goes up to 5 dB for NC4. Interestingly, the JPAPS keeps on having an advantage of 2 dB for both NC3 and NC4 also against the cooperative DF-CR-EP, in spite of requiring a much lower complexity.

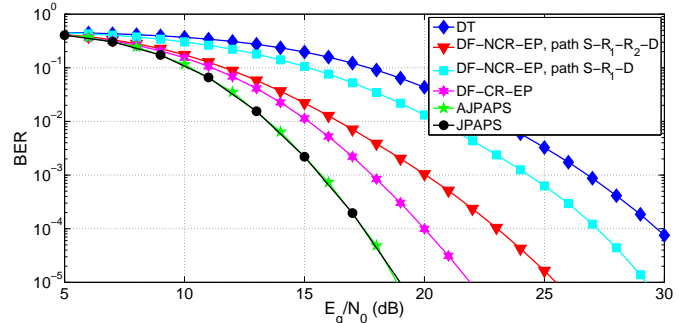


Fig. 8. BER as a function of the SNR for various transmission schemes (NC3).

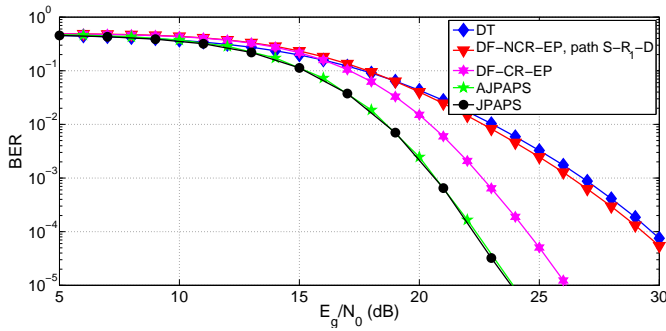


Fig. 9. BER as a function of the SNR for various transmission schemes (NC4).

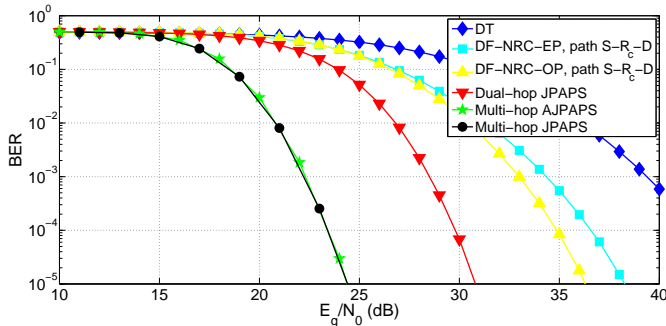


Fig. 10. BER as a function of the SNR for various transmission schemes (NC5).

As the last test case, Figure 10 refers to the configuration NC5 in which up to  $N = 10$  relays can be adopted by the transmission schemes. To be specific, the DF-NCR-OP scheme that employs the path  $\mathcal{P}(S, R_c, D)$ , where  $R_c$  is the relay located at the center of the square, exhibits a gain of more than 6 dB compared to the DT, while, without optimizing the PA coefficients, the advantage on the direct transmission reduces to 5 dB. Notice that the proposed JPAPS, even when only one relay can be used, brings an additional performance gain of 4.5 dB relative to the DF-NCR-OP, which always adopts the relay  $R_c$ . Then, if all the relays are available for transmission, the multi-hop JPAPS (and also its approximated version) considerably outperforms the dual-hop JPAPS scheme by more than 6 dB.

Hence, the results obtained for the multi-hop scenarios corroborate the effectiveness of the proposed JPAPS and AJPAPS techniques, which show remarkable gains compared to the benchmark schemes specified in Sect. V-A.

## VI. CONCLUDING REMARKS

In this paper, we presented a differentially encoded DF non-cooperative relaying scheme suited for noncoherent multi-hop UWB communication systems. The key of the approach relies on a novel joint power allocation and path selection algorithm, referred to as JPAPS. Given a relaying path, we firstly showed how to distribute near-optimal power coefficients in closed form via an equal-SNR strategy. Then, the

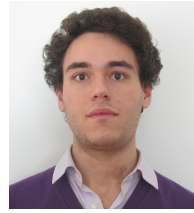
optimal path minimizing a proper approximation of the overall BER has been chosen by means of a two-step procedure with complexity  $\mathcal{O}(N^3)$ , where  $N$  is the number of relays of the network. In addition, an approximated algorithm running in  $\mathcal{O}(N^2)$  has been developed through a reformulation of the path selection problem into a shortest path search on a connected graph. The proposed relaying scheme does not require any information on the network topology, but only the energies captured by the bandpass filters at the receivers of the nodes. Extensive simulation results conducted over typical wireless environments for various network setups prove the excellent performance achieved by the JPAPS algorithm in its exact and approximated version, thus outperforming the existing AF and DF relaying schemes.

Further, under the typical assumptions of high-SNR regime and channel time invariance within the transmitted block, a potential of the proposed JPAPS method lies on the considerable fact that it can be generally applied not only to the context of multi-hop UWB communications, but also to the case of a generic relaying network, wherein the transmitters employ single carrier (SC) differentially encoded modulation and the receivers recover information symbols via noncoherent demodulation. Concerning, instead, the more demanding case of multicarrier (MC) systems such as, for example, orthogonal frequency division multiplexing (OFDM) or filter-bank MC (FBMC), the application of the JPAPS scheme is possible but not so immediate, and accordingly, it will be interestingly addressed in future works.

## REFERENCES

- [1] M. Z. Win and R. A. Scholtz, "Ultra-wide bandwidth time-hopping spread-spectrum impulse radio for wireless multiple-access communications," *IEEE Trans. on Commun.*, vol. 48, no. 4, pp. 679–689, Apr. 2000.
- [2] G. B. Giannakis and L. Yang, "Ultra-wideband communications: an idea whose time has come," *IEEE Signal Process. Mag.*, vol. 21, no. 6, pp. 26–54, Nov. 2004.
- [3] S. Roy, J. R. Foerster, V. S. Somayazulu, and D. G. Leeper, "Ultrawideband radio design: the promise of high-speed, short-range wireless connectivity," *Proc. of IEEE*, vol. 92, no. 2, pp. 295–311, Feb. 2004.
- [4] M. Z. Win and R. A. Scholtz, "On the energy capture of ultrawide bandwidth signals in dense multipath environments," *IEEE Commun. Lett.*, vol. 2, no. 9, pp. 245–247, Sept. 1998.
- [5] M. Z. Win, G. Chrisikos, and N. R. Sollenberger, "Performance of RAKE reception in dense multipath channels: implications of spreading bandwidth and selection diversity order," *IEEE J. Sel. Areas Commun.*, vol. 18, no. 8, pp. 1516–1525, Aug. 2000.
- [6] V. Lottici, A. D'Andrea, and U. Mengali, "Channel estimation for ultrawideband communications," *IEEE J. Sel. Areas Commun.*, vol. 20, no. 9, pp. 1638–1645, Dec. 2002.
- [7] Federal Communications Commission (FCC), "First report and order in the matter of revision of part 15 of the commissions rules regarding ultra-wideband transmission systems," *Tech. Rep. ET Docket 98-153*, Apr. 2002.
- [8] J. N. Laneman, D. N. C. Tse, and G. W. Wornell, "Cooperative diversity in wireless networks: efficient protocols and outage behavior," *IEEE Trans. on Inf. Theory*, vol. 50, no. 12, pp. 3062–3080, Dec. 2004.
- [9] L. Le and E. Hossain, "Multihop cellular networks: potential gains, research challenges, and a resource allocation framework," *IEEE Commun. Mag.*, vol. 45, no. 9, pp. 66–73, Sept. 2007.

- [10] T. C. Y. Ng and W. Yu, "Joint optimization of relay strategies and resource allocations in cooperative cellular networks," *IEEE J. Sel. Areas Commun.*, vol. 25, no. 2, pp. 328–339, Feb. 2007.
- [11] A. Bletsas, A. Khisti, D. P. Reed, and A. Lippman, "A simple cooperative diversity method based on network path selection," *IEEE J. Sel. Areas Commun.*, vol. 24, no. 3, pp. 659–672, Mar. 2006.
- [12] K. Maichalernnukul, T. Kaiser, and F. Zheng, "On the performance of coherent and noncoherent UWB detection systems using a relay with multiple antennas," *IEEE Trans. on Wireless Commun.*, vol. 8, no. 7, pp. 3407–3414, Jul. 2009.
- [13] C. Abou-Rjeily, N. Daniele, and J.-C. Belfiore, "On the amplify-and-forward cooperative diversity with time-hopping ultra-wideband communications," *IEEE Trans. on Commun.*, vol. 56, no. 4, pp. 630–641, Apr. 2008.
- [14] S. Zhu, K. K. Leung, and A. G. Constantinides, "Distributed cooperative data relaying for diversity in impulse-based UWB ad-hoc networks," *IEEE Trans. on Wireless Commun.*, vol. 8, no. 8, pp. 4037–4047, Aug. 2009.
- [15] K. Witrisal, G. Leus, G. J. M. Janssen, M. Pausini, F. Troesch, T. Zasowski, and J. Romme, "Noncoherent ultra-wideband systems," *IEEE Signal Process. Mag.*, vol. 26, no. 4, pp. 48–66, Jul. 2009.
- [16] M. Ho, V. S. Somayazulu, J. Foerster, and S. Roy, "A differential detector for an ultra-wideband communications system," in *Proc. IEEE Veh. Tech. Conf.*, May 2002, pp. 1896–1900.
- [17] R. Hoor and H. Tomlinson, "Delay-hopped transmitted-reference RF communications," in *Proc. IEEE Ultra Wideband Syst. Tech. Conf.*, May 2002, pp. 265–269.
- [18] Y.-L. Chao and R. A. Scholtz, "Optimal and suboptimal receivers for ultra-wideband transmitted reference systems," in *Proc. IEEE Global Telecommun. Conf.*, Dec. 2003, pp. 759–763.
- [19] Z. Wang, T. Lv, H. Gao, and Y. Li, "A novel two-way relay UWB network with joint non-coherent detection in multipath," in *Proc. IEEE Veh. Tech. Conf.*, May 2011, pp. 1–5.
- [20] M. Hamdi, J. Mietzner, and R. Schober, "Multiple-differential encoding for multi-hop amplify-and-forward IR-UWB systems," *IEEE Trans. on Wireless Commun.*, vol. 10, no. 8, pp. 2577–2591, Aug. 2011.
- [21] M. Mondelli, Q. Zhou, X. Ma, and V. Lottici, "A cooperative approach for amplify-and-forward differential transmitted reference IR-UWB relay systems," in *Proc. IEEE Int. Conf. Acoust., Speech, and Signal Proc.*, Mar. 2012, pp. 2905–2908.
- [22] I. Stojmenovic, "Position-based routing in ad hoc networks," *IEEE Commun. Mag.*, vol. 40, no. 7, pp. 128–134, Jul. 2002.
- [23] M. R. Casu and G. Durisi, "Implementation aspects of a transmitted-reference UWB receiver," *Wireless Commun. and Mobile Computing*, vol. 5, no. 5, pp. 537–549, Aug. 2005.
- [24] L. Feng and W. Namgoong, "An oversampled channelized UWB receiver with transmitted reference modulation," *IEEE Trans. Wireless Commun.*, vol. 5, no. 6, pp. 1497–1505, Jun. 2006.
- [25] A. F. Molisch, "Ultra-wide-band propagation channels," *Proc. of IEEE*, vol. 97, no. 2, pp. 353–371, Feb. 2009.
- [26] S. Boyd and L. Vandenberghe, *Convex optimization*, Cambridge University Press, New York, USA, 2004.
- [27] R. Guerin and A. Orda, "Computing shortest paths for any number of hops," *IEEE/ACM Trans. on Networking*, vol. 10, no. 5, pp. 613–620, Oct. 2002.
- [28] M. L. Fredman and R. E. Tarjan, "Fibonacci heaps and their uses in improved network optimization algorithms," *Journal of the ACM*, vol. 34, no. 3, pp. 596–615, Jul. 1987.
- [29] J. Foerster, "Channel modeling sub-committee report final," Tech. Rep., IEEE P802.15-02/490r1-SG3a, Feb. 2003.
- [30] K. Dhaka, R. K. Mallik, and R. Schober, "Optimisation of power allocation for asymmetric relay placement in multi-hop relay systems," *IET Communications*, vol. 7, no. 2, pp. 128–136, Jan. 2013.



**Marco Mondelli** received the B.S. and M.S. degree in Telecommunications Engineering from the University of Pisa, Italy, in 2010 and 2012, respectively. During the period 2007–2012, he was dually enrolled at the Sant'Anna School of Advanced Studies on a full 5 years scholarship. He joined as an intern the École Normale Supérieure de Cachan in March–April 2010 and the Georgia Institute of Technology in August–November 2012. Since September 2012, he is working towards the Ph.D. degree in Computer, Communication and Information Sciences at the

École Polytechnique Fédérale de Lausanne, Switzerland, where he is advised by Prof. Rüdiger Urbanke. His current research interests include wireless communications, especially as concerns ultra-wideband systems and relaying networks, network information theory and coding, with particular emphasis on polar codes.



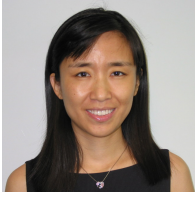
**Qi Zhou (S'10)** received the B.S. degree in Mathematics and Applied Mathematics from the Beijing University of Posts and Telecommunications, Beijing, P. R. China, in 2006, the M.S. degree in Computer Science from Shanghai Jiaotong University, Shanghai, P. R. China, in 2009, the M.S. degree in Electrical and Computer Engineering from the Georgia Institute of Technology, Atlanta, GA, in 2009, and the Ph.D. degree in Electrical and Computer Engineering from the Georgia Institute of Technology, Atlanta, GA, in 2013. He is now

with Matrix Technologies, Atlanta, GA. His current research interests include transceiver designs for ultra-wideband communications, interference mitigation for femtocell/macrocen networks, equalizations for large multiple-input multiple-output systems, and VLSI implementation of energy-efficient high-throughput detectors.



**Vincenzo Lottici** received the Dr. Ing. degree (cum Laude) and the BTA in electrical engineering both from the University of Pisa in 1985 and 1986, respectively. From 1987 to 1993 he was engaged in the research of sonar digital signal processing algorithms. Since 1993 he has been with the Department of Information Engineering of the University of Pisa, where he is currently an Assistant Professor in Communication Systems. He participated in several international and national research projects, and as TPC member, in numerous

IEEE conferences in wireless communications and signal processing, such as Globecom2013, WCNC2013, ICUWB2013, WCNC2012, ICUWB2011, ICC2011, WCNC2011, ICASSP2010, PIMRC2010, WCNC2010, CIP2010, Globecom2009, SPAWC2009, EUSIPCO2006, Globecom2006. He joined the Editorial Board of EURASIP Advances on Signal Processing. Dr. Lottici received the Best Paper Award in 2006 for the work "A Theoretical Framework for Soft Information Based Synchronization in Iterative (Turbo) Receivers", EURASIP Journal on Wireless Communications and Networking, April 2005, by the EU-funded project Network of Excellence in Wireless Communications (NEWCOM). His research interests include the broad area of signal processing for communications, with emphasis on synchronization, dynamic resource allocation, cognitive radio and compressive sensing.



**Xiaoli Ma (SM'09)** received the B.S. degree in automatic control from Tsinghua University, Beijing, China in 1998, the M.S. degree in electrical engineering from the University of Virginia, Charlottesville, in 2000, and the Ph.D. degree in electrical engineering from the University of Minnesota, Minneapolis, in 2003. From 2003 to 2005, she was an Assistant Professor of Electrical and Computer Engineering at Auburn University. Since 2006, she has been with the School of Electrical and Computer Engineering at Georgia Institute of Technology, Atlanta, where she is currently an Associate Professor. Her research interests include transceiver designs and diversity techniques for wireless fading channels, cooperative communications, UWB communications, synchronization for multi-carrier systems, and channel modeling, estimation, and equalization for wireless systems.